AJNR

Investigating Sea-Level Brain Predictors for Acute Mountain Sickness: A Multimodal MRI Study before and after High-Altitude Exposure

Wei Zhang, Jie Feng, Wenjia Liu, Shiyu Zhang, Xiao Yu, Jie Liu, Baoci Shan and Lin Ma

AJNR Am J Neuroradiol 2024, 45 (6) 809-818
doi: https://doi.org/10.3174/ajnr.A8206
http://www.ajnr.org/content/45/6/809

Investigating Sea-Level Brain Predictors for Acute Mountain Sickness: A Multimodal MRI Study before and after High-Altitude Exposure

Wei Zhang, Jie Feng, Wenjia Liu, Shiyu Zhang, Xiao Yu, Jie Liu, Baoci Shan, and Lin Ma

ABSTRACT

BACKGROUND AND PURPOSE: Acute mountain sickness is a series of brain-centered symptoms that occur when rapidly ascending to high altitude. Predicting acute mountain sickness before high-altitude exposure is crucial for protecting susceptible individuals. The present study aimed to evaluate the feasibility of predicting acute mountain sickness after high-altitude exposure by using multimodal brain MR imaging features measured at sea level.

MATERIALS AND METHODS: We recruited 45 healthy sea-level residents who flew to the Qinghai-Tibet Plateau (3650 m). We conducted T1-weighted structural MR imaging, resting-state fMRI, and arterial spin-labeling perfusion MR imaging both at sea level and high altitude. Acute mountain sickness was diagnosed for 5 days using Lake Louise Scoring. Logistic regression with Least Absolute Shrinkage and Selection Operator logistic regression was performed for predicting acute mountain sickness using sea-level MR imaging features. We also validated the predictors by using MR images obtained at high altitude.

RESULTS: The incidence rate of acute mountain sickness was 80.0%. The model achieved an area under the receiver operating characteristic curve of 86.4% (sensitivity = 77.8%, specificity = 100.0%, and $P < .001$) in predicting acute mountain sickness At sea level, valid predictors included fractional amplitude of low-frequency fluctuations (fALFF) and degree centrality from resting-state fMRI, mainly distributed in the somatomotor network. We further learned that the acute mountain sickness group had lower levels of fALFF in the somatomotor network at high altitude, associated with smaller changes in CSF volume and higher Lake Louise Scoring, specifically relating to fatigue and clinical function.

CONCLUSIONS: Our study found that the somatomotor network function detected by sea-level resting-state fMRI was a crucial predictor for acute mountain sickness and further validated its pathophysiologic impact at high altitude. These findings show promise for pre-exposure prediction, particularly for individuals in need of rapid ascent, and they offer insight into the potential mechanism of acute mountain sickness.

ABBREVIATIONS: AMS = acute mountain sickness; ASL = arterial spin-labeling; AUC = area under the curve; DC = degree centrality; fALFF = fractional amplitude of low-frequency fluctuations; LASSO-LR = Least Absolute Shrinkage and Selection Operator logistic regression; LLS = Lake Louise Score; rs-fMRI = resting-state fMRI; ROC = receiver operating characteristic; SMN = somatomotor network; SpO_2 = saturation of pulse oxygen

Approximately 25%–90% of sea-level residents who travel to high altitude will have acute mountain sickness (AMS), depending on the altitude, the speed of ascent, and individual susceptibility.[1] AMS is a series of symptoms including headache, dizziness, and malaise. It can even lead to incapacitation or life-threatening conditions such as high-altitude cerebral edema and pulmonary edema.[2]

It was recommended that high-altitude travelers have medical consulting regarding AMS before exposure.[3] Predicting AMS

Received November 20, 2023; accepted after revision January 23, 2024.

From the Beijing Engineering Research Center of Radiographic Techniques and Equipment (W.Z., B.S.), Institute of High Energy Physics, Chinese Academy of Sciences, Beijing, China; School of Nuclear Science and Technology (W.Z., B.S.), University of Chinese Academy of Sciences, Beijing, China; The Graduate School (J.F., X.Y., L.M.), Medical School of Chinese People's Liberation Army, Beijing, China; Department of Radiology (J.F., W.L., S.Z., X.Y., L.M.), The First Medical Center of Chinese People's Liberation Army General Hospital, Beijing, China; Department of Radiology (S.Z.), Capital Medical University Affiliated Beijing Friendship Hospital, Beijing, China; Department of Radiology (X.Y.), Beijing Jingmei Group General Hospital, Beijing, China; Department of Radiology (J.L.), General Hospital of Tibet Military Region, Tibet, China; and Cognitive Neuroimaging Centre (W.Z.) and Lee Kong Chian School of Medicine (W.Z.), Nanyang Technological University, Singapore.

W. Zhang and J. Feng contributed equally to this work.

This work was supported by National Natural Science Foundation of China, grant No. 81741115, 81771923, 11975249, and 12175268, Chinese Military Creative Project, grant No. 16CXZ014, Chinese Military Healthcare, grant No. 16BJZ11.

Please address correspondence to Lin Ma, MD, Department of Radiology, The First Medical Center of Chinese People's Liberation Army General Hospital, 28 Fuxing Road, Beijing 100853, China; e-mail: cjr.malin@vip.163.com

Indicates article with online supplemental data.

http://dx.doi.org/10.3174/ajnr.A8206

before exposure is also essential for protecting individuals from greater health risks. Because rapid ascent is a risk factor of AMS,[1] individuals requiring rapid ascent to high-altitude areas might particularly need the prediction, such as those undertaking urgent high-altitude missions like disaster relief, medical rescue, and some scientific investigations. Currently, 2 main factors show promise in predicting AMS: the history of AMS and migraine[4] and the adaptation performance in moderate hypoxia, such as the cardiopulmonary function in artificial hypoxic environments[4-7] and adaptation extents at moderate altitudes.[8-12] However, the prediction performance was inconsistent and debated, because studies have reported conflicting results using the same predictors.[13-16] Furthermore, most individuals have limited high-altitude experience, making prediction based on history less feasible. The artificial hypoxic environments, often requiring specialized labs, are also debated for not adequately replicating the hypobaric conditions of real high altitude.[17]

The inconsistent performance in predicting AMS may be due to an incomplete understanding of the mechanisms.[18] Among the hypotheses, the brain plays a key role in both human and animal research.[19,20] The physiologic adaptation after high-altitude exposure is brain-centered and crucial for the onset of AMS, which is hypothesized to involve multiple neural processes such as the perception and processing of the sensory information from a high-altitude environment[21,22] and the activation of the autonomic neural system.[23,24] The swelling of gray and white matter, the morphologic changes of the cortex, the restricted outflow of CSF, and the increased CBF can increase intracranial pressure and thus cause AMS,[25,26] while the contributions of different components toward AMS are still debated.[27] Those hypotheses involve multiple aspects of the brain, including function, structure, and perfusion. However currently, multimodal MR imaging studies for AMS scanned at both sea level and high altitude are still rare and have not involved integrated pre-exposure prediction.[28,29] The feasibility of using multimodal MR imaging to investigate and predict AMS requires further verification.

In this study, we arranged for 45 participants to fly from sea level to the Qinghai-Tibet Plateau. They underwent 3 modalities of MR imaging twice (before and after high-altitude exposure) and were diagnosed as having AMS or non-AMS. On the basis of the previous studies, we hypothesized that the AMS group would have distinct cerebral features at sea level, detectable by multimodal MR imaging, and that we could further investigate its pathophysiologic impact using MR imaging after exposure.

MATERIALS AND METHODS

Study Design

This study was conducted in both sites of the Chinese People's Liberation Army General Hospital (Beijing, at sea level) and The General Hospital of Tibet Military Region (Lhasa, 3650 m above sea level). In Beijing as a baseline, participants were scanned by 3 modalities: T1-weighted imaging, resting-state fMRI (rs-fMRI), and arterial spin-labeling (ASL) perfusion MR imaging. Then, participants traveled to Lhasa via commercial flights within 2 days. In Lhasa, participants underwent the same MR imaging protocol at 22 hours and were diagnosed as either having AMS or not having AMS during the first 5 days at the following time points: 9, 22, 46, 70, and 94 hours. The flow chart of the study design is shown in Fig 1*A*. Demographic and physiologic features were recorded at baseline for prediction.

Participants

A total of 49 participants were recruited through community advertising. Four participants were excluded due to strong head-motion artifacts on MR imaging at baseline, identified after post hoc checking. Two rs-fMRIs from the 45 participants at high altitude were excluded due to poor image quality, but sea-level data from these 2 participants were still valid and included for prediction.

The recruitment criteria were as follows: 1) 20–40 years of age; 2) no history of severe head trauma, chronic headache, chronic sleep disorders, other neuropathy, or psychosis; 3) nonsmokers and not abusing alcohol; 4) not taking any prescription or nonprescription medications at the time of the study; 5) no chronic heart or lung disease, diabetes, hypertension, or other basic diseases; 6) right-handed; 7) originally from and currently residing at sea level and not having traveled to an altitude above 1500 m in the past year; and 8) no carotid or intracranial vascular lesions detected by MRA.

AMS Diagnosis

The AMS diagnosis is based on the latest Lake Louise scoring.[30] Participants with a headache score of $\geq$1 and a Lake Louise Score (LLS) of $\geq$ 3 were diagnosed with AMS on a daily basis. Participants diagnosed with AMS at least once during the 5 days at high altitude were grouped as having AMS. The LLS is composed of 4 main different subscores: 1) headache, 2) gastrointestinal symptoms, 3) fatigue and/or weakness, and 4) dizziness/light-headedness. The extra subscore, the clinical-functional score, was used to evaluate the overall impact on patients with AMS but is not included in the total score.

Multimodal MR Imaging Acquisitions and Preprocessing

MR imaging was performed using a 3T Discovery MR 750 scanner (GE Healthcare) both at sea level and high altitude to minimize variance caused by scanner differences.

T1-weighted structural MR imaging was acquired using the 3D fast-spoiled gradient recalled protocol with the following parameters: TR = 6.9 ms, TE = 3.0 ms, TI = 450 ms, flip angle = 12°, FOV = 25.6 cm, 188 slices with section thickness = 1 mm, matrix = 256 × 256, voxel resolution = 1 mm, and number of excitations = 1.

rs-fMRI was acquired measuring blood oxygenation level–dependent signals with an EPI sequence: TR = 2000 ms, TE = 30 ms, flip angle = 90°, FOV = 24.0 cm, 41 slices with section thickness = 3 mm, matrix = 64 × 64, voxel resolution = 3.75 mm, and time-series length = 240.

For pseudocontinuous ASL perfusion images, the labeling duration = 1.5 seconds, postlabel delay = 2.0 seconds, TR = 4844 ms, TE = 10.5 ms, TI = 2025 ms, flip angle = 111°, bandwidth = 62.5 kHz, FOV = 24 cm, 36 slices with section thickness = 4 mm, acquisition matrix = 128 × 128, resolution = 1.875 mm, and number of excitations = 3. The proton density–weighted images

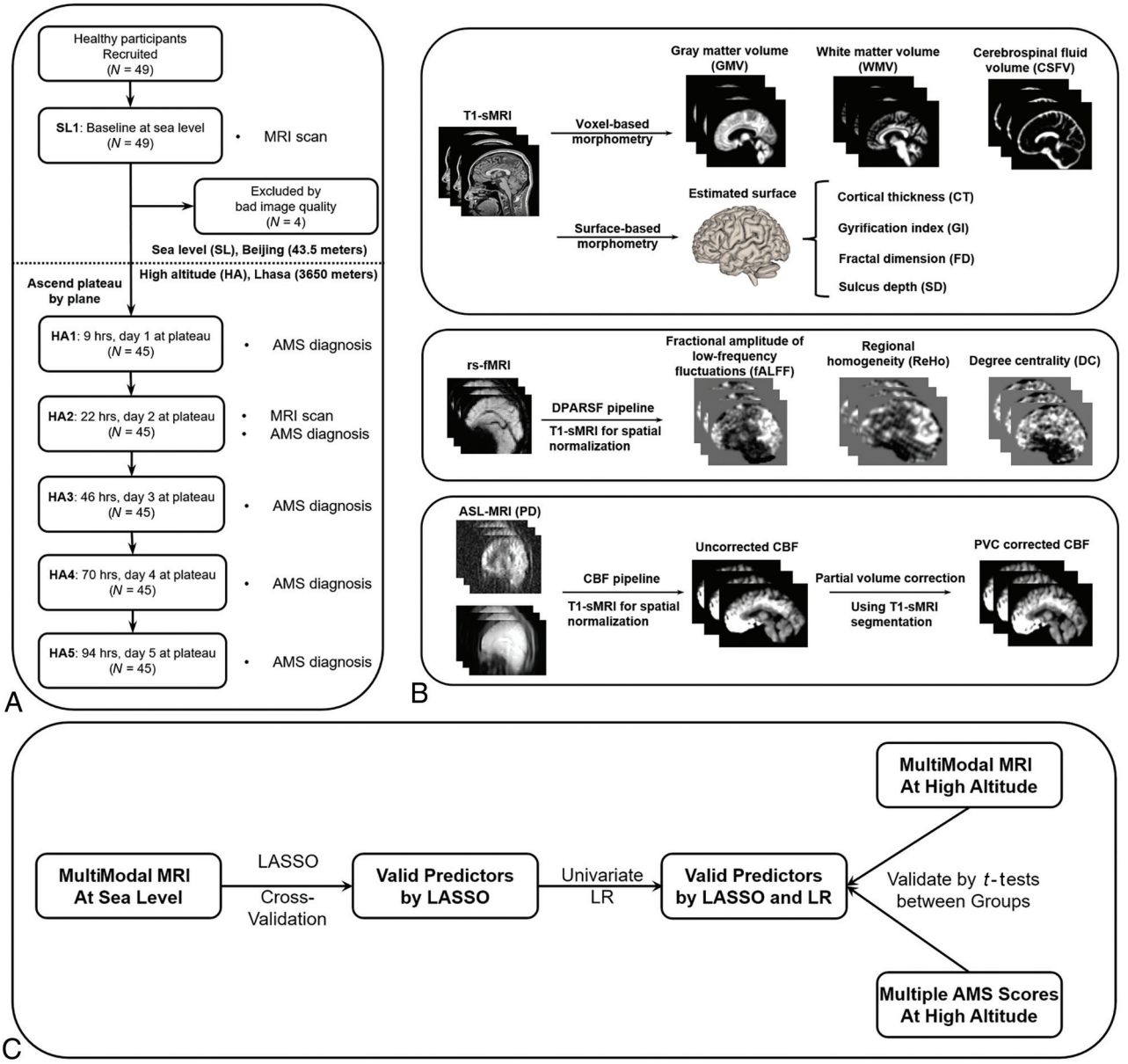

FIG 1. The study design and the analysis pipelines for multimodal MR images. *A*, The study design. Participants were recruited and underwent MR imaging at sea level, ascended to the high altitude by plane, were scanned by MR imaging at 22 hours, and evaluated for AMS 5 times at high altitude. *B*, Multimodal MR imaging preprocessing. Different preprocessing pipelines produced 11 features from 3 modalities of MR imaging, and these features were further summarized by the mean value in ROIs. *C*, Feature selection. The sea-level MR imaging features for prediction of AMS were selected by LASSO-LR and re-verified by univariate logistic regression. Sea-level predictors were subsequently verified using high-altitude MR imaging and AMS scores (LLS) collected at high altitude. DPARSF indicates Data Processing Assistant for Resting-State fMRI; LR, logistic regression; PD, proton density–weighted images; PVC, partial volume correction.

were obtained with a saturation recovery acquisition with identical parameters.

A summary of the multimodal MR imaging preprocessing pipeline is shown in Fig 1*B*. We have summarized the preprocessing steps and features extracted for each technique in Table 1. For detailed preprocessing steps, refer to the Online Supplemental Data.

Prediction Input and Methods

The sea-level MR imaging features were summarized by the mean values in ROIs from the Automated Anatomical Labeling atlas[31] (https://www.sciencedirect.com/science/article/pii/S1053811919307803) or the surface atlas[32] and were used as prediction input. Sea-level demographic and physiologic features were also entered as potential confounding covariates.

For the prediction methods, we used the Least Absolute Shrinkage and Selection Operator[33] logistic regression (LASSO-LR) due to its capability for feature selection (detailed implementation is in the Online Supplemental Data). We applied the leave-one-out framework for cross-validation.

We primarily evaluated the final prediction performance using the area under the curve (AUC) of the receiver operating

Table 1: Preprocessing and features of multimodal MR imaging

Technique	Preprocessing Pipeline	Main Preprocessing Steps	Features after Preprocessing	ROI No.
T1-sMRI (volume)	Voxel-based morphometry	Denoising, bias cleaning, affine registration, segmentation, spatial normalization, volume modulation, smoothing	GM volume	166
			WM volume	166
			CSF volume	166
T1-sMRI (surface)	Surface-based morphometry	Surface reconstruction, cortical parcellation, spatial normalization, smoothing	Cortical thickness	68
			Gyrification index	68
			Fractal dimension	68
			Sulcus depth	68
Rs-fMRI	DPARSF standard preprocessing pipeline	Time point removal, section timing, realignment, affine registration, nuisance regression, head motion correction, spatial normalization, metric calculation, smoothing	fALFF	166
			Regional homogeneity	166
			DC	166
ASL	CBF quantification pipeline	Coregistration, CBF calculation, partial volume correction, spatial normalization, whole-brain normalization, smoothing	CBF	166

Note:—DPARSF indicates Data Processing Assistant for Resting-State fMRI (Matlab); sMRI, structural MR imaging.

Table 2: Demographic and physiologic features for the AMS and non-AMS groups at sea-level baseline[a]

	Non-AMS ($n = 9$)	AMS ($n = 36$)	*P* Value
Age (yr)	27.3 (SD, 3.8)	29.4 (SD, 4.6)	.1497
Sex (M/F)	5/4	17/19	.1779
Height (cm)	168.9 (SD, 6.5)	168.4 (SD, 8.5)	.8776
Weight (kg)	61.1 (SD, 8.0)	64.7 (SD, 13.3)	.4462
BMI (kg/m^2)	21.4 (SD, 2.3)	22.6 (SD, 3.2)	.2848
SBP (min^{-1})	111.3 (SD, 12.1)	111.9 (SD, 12.4)	.9094
DBP (min^{-1})	75.1 (SD, 8.1)	75.6 (SD, 8.7)	.8703
MAP (min^{-1})	87.2 (SD, 9.2)	87.7 (SD, 9.6)	.8823
HR (min^{-1})	74.3 (SD, 7.2)	74.1 (SD, 8.1)	.9402
SpO_2 (%)	97.8 (SD, 0.8)	97.6 (SD, 0.7)	.4137

Note:—BMI indicates body mass index; DBP, diastolic blood pressure; HR, heart rate; MAP, mean arterial pressure; SBP, systolic blood pressure.
[a] Data are means unless otherwise indicated.

characteristic (ROC) because of the unbalanced labels (36 AMS of 45 participants). The ROC is suitable for measuring the classification performance on unbalanced labels[34-36] because it is generated across a range of decision thresholds and is less sensitive to unbalanced label distribution. Sensitivity and specificity were also calculated at the cut-point of the best Youden index. All prediction methods were implemented using the scikit-learn toolbox, Version 1.0.2 (https://scikit-learn.org/stable/index.html).

Statistical Analyses

For investigating the valid predictors, we performed the feature-selection pipeline shown in Fig 1C. Specifically, we accepted valid predictors that passed both multivariate LASSO-LR and univariate logistic regressions.

T tests were performed to compare image features between groups. Because the predictors are regionally averaged, we further reverified them by detecting group differences between AMS and non-AMS at both voxelwise and network-wise scales, using MR imaging data from both sea level and high altitude.

All features were converted to a standard normal *z* score before prediction and statistical analyses.

The voxelwise analysis of MR images was performed on the basis of Statistical Parametric Mapping (SPM 12;http://www.fil.ion.ucl.ac.uk/spm/software/spm12). The network-wise *t* tests between groups used the predefined brain network atlas (https://surfer.nmr.mgh.harvard.edu/fswiki/CorticalParcellation_Yeo2011).[37] This atlas was used to re-verify the regional predictors and to detect potential networks involved. A partial Pearson correlation was used to assess the relationship between MR imaging predictors and other brain features they might influence. Before the statistical tests mentioned above, the values were regressed by the covariates of age and sex to exclude their potential effects. The statistical analyses were performed using related in-house scripts in Matlab (MathWorks).

RESULTS

Incidence Rate of AMS

The demographic and physiologic information at sea-level baseline is provided in Table 2, and no significant difference between AMS and non-AMS groups was detected using *t* tests and χ^2 tests.

The overall incidence rate of AMS during 5 days was 80.0% (36 of 45 participants; 95% CI , 66.7%–1.1%). The daily incidence rates of AMS were as follows: 66.7% at 9 hours after exposure (95% CI, 51.1%–80.0%), 48.9% at 22 hours (95% CI, 33.3%–64.4%), 46.7% at 46 hours (95% CI, 31.2%–62.2%), 31.1% at 70 hours (95% CI, 17.8%–46.7%), and 17.8% at 94 hours (95% CI, 6.7%–28.9%). Individual AMS diagnoses are provided in the Online Supplemental Data.

Prediction of AMS Using Multimodal Sea-Level MR Imaging

We used each type of feature in ROIs from sea-level multimodal MR imaging to predict AMS at high altitude (Fig 2, and with Youden cutoff in the Online Supplemental Data). Two fMRI metrics showed significant predictive performance: for fALFF as input, AUC = 78.1%, sensitivity = 80.5%, and specificity = 77.8% ($P = .0098$) and for degree centrality (DC) as input, AUC = 86.4%, sensitivity = 77.8%, and specificity = 100.0%

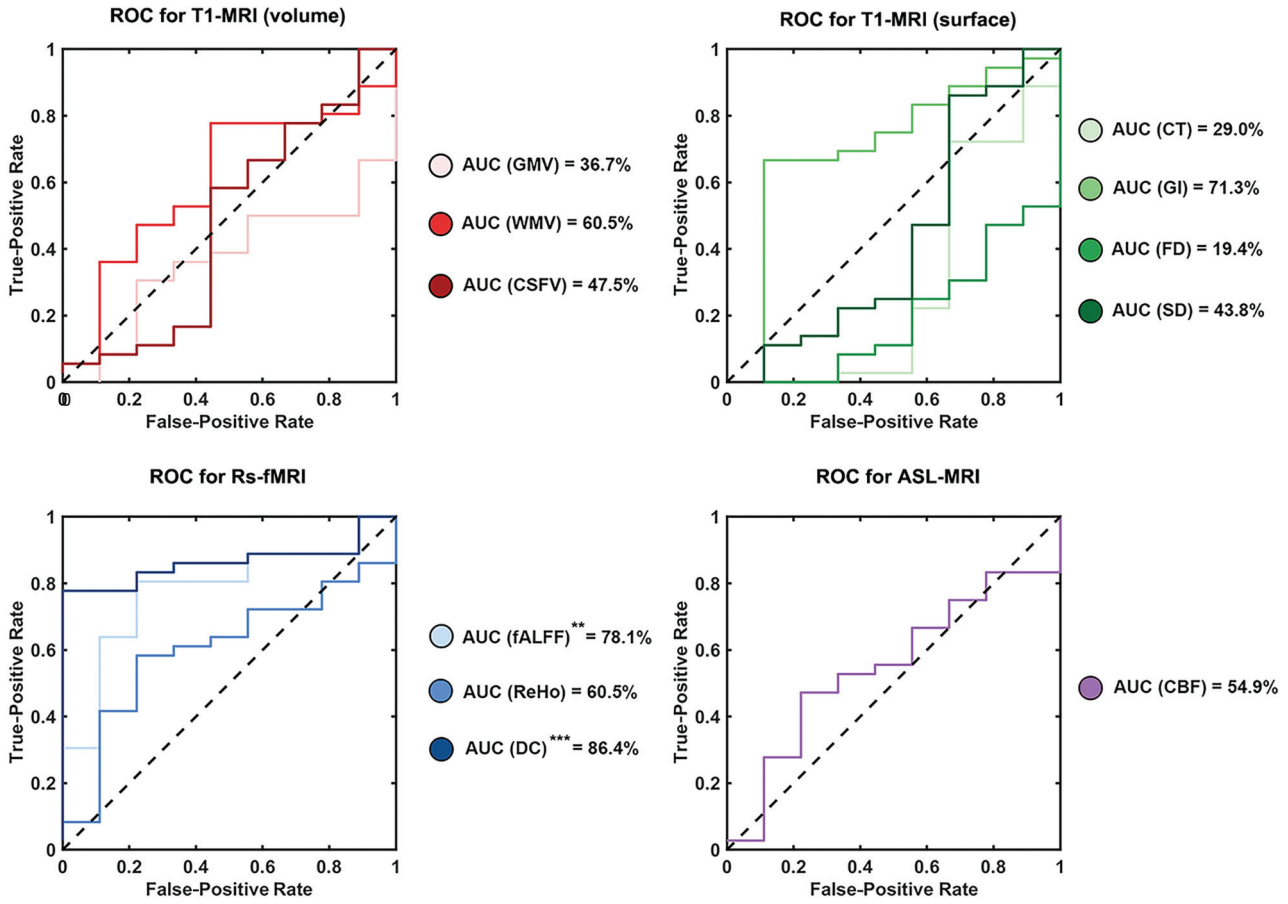

FIG 2. ROC curve analysis of MR imaging features. The prediction performance using different features of multimodal MR imaging as input, measured by the AUC of the ROC curves. fALFF and DC from fMRI were detected as valid predictors, yielding significant AUC values. CT indicates cortical thickness; FD, fractal dimension; GI, gyrification index; GMV, gray matter volume; ReHo, regional homogeneity; SD, sulcus depth; WMV, white matter volume, CSFV, CSF volume. ** $P < .01$, *** $P < .001$.

($P = .0008$). Other input features had no significant predictive performance, including combined features (such as all fMRI features or all multimodal MR imaging features). The full performance list of all types of input is provided in the Online Supplemental Data.

Identification and Verification of Sea-Level MR Imaging Predictors

Following the predictions, sea-level predictors were identified from the multivariate LASSO-LR. Then, these potential predictors were re-verified by univariate logistic regression, and only those that passed both regressions were regarded as valid predictors. Valid predictors were fALFF and DC values in the regions listed in Table 3.

Among the valid predictors, risk factors with ORs > 1 were mainly located in the orbitofrontal cortex and the right supramarginal gyrus. Protective factors with odds ratios < 1 were mainly located in the paracentral lobule, supplementary motor area, and Rolandic operculum, all of which belonged to the somatomotor network (SMN). The left superior and middle temporal gyri were also included as protective factors, which were near the Rolandic operculum. These predictors selected by the LASSO-LR models remained robust during the leave-one-out cross-validation (Online Supplemental Data).

Predictors of AMS Present in the SMN Both at Sea Level and High Altitude

To further verify the region-wise predictors, we performed voxel-wise *t* tests between groups on the fMRI metrics (fALFF and DC) maps. Both at sea level and at high altitude, the AMS group showed weaker functional metrics mainly in the motor and sensorimotor areas (Fig 3*A*, -*C*) than the non-AMS group (under $P < .05$, corrected by Gaussian random field).

We further verified the region-wise predictors by detecting network-wise group difference on the *z*-scored fMRI metric (fALFF and DC) maps using a predefined atlas.[37] At sea level (Fig 3*B*), the significant functional group difference in the predefined SMN between the AMS and non-AMS groups was detected by *t* tests: For fALFF, the AMS group showed significantly ($P = .0082$) lower values than the non-AMS group in the SMN (mean AMS) = −0.2095 (SD, 0.1613), mean (non-AMS) = 0.8381 (SD, 0.2140), group difference = 1.0476 (95% CI , 0.3590–1.7362). Similarly, for DC, the AMS group had significantly ($P = .0424$) lower values than the non-AMS group in the SMN (mean AMS) = −0.1706 (SD, 0.1632), mean (non-AMS) = 0.6824 (SD, 0.2693), group difference = 0.8529 (95% CI, 0.1394−1.5665). At high altitude (Fig 3*D*), for fALFF, the AMS group showed significantly ($P = .0320$) lower values than the non-AMS group in the SMN (mean AMS) = −0.1486 (SD, 0.1685), mean (non-AMS) = 0.5615 (SD, 0.3019), group

Table 3: ORs of significant predictors for AMS, selected by both the LASSO-LR and univariate logistic regression

Input Features/Input Regions	B	OR (95% CI)	*P* Value
fALFF			
Left Rolandic operculum	−1.324	0.266 (0.091–0.778)	.0157
Left supplementary motor area	−1.931	0.145 (0.025–0.857)	.0331
Right superior frontal gyrus, medial orbital	1.272	3.567 (1.207–10.543)	.0214
Right anterior orbital gyrus	0.852	2.344 (1.049–5.236)	.0379
Right supramarginal gyrus	1.288	3.624 (1.296–10.139)	.0141
Left paracentral lobule	−2.727	0.065 (0.009–0.488)	.0078
Left superior temporal gyrus	−1.040	0.354 (0.150–0.836)	.0179
Left middle temporal gyrus	−1.367	0.255 (0.081–0.803)	.0196
Right pulvinar inferior thalamus	0.894	2.445 (1.014–5.895)	.0466
DC			
Right superior frontal gyrus, dorsolateral	1.363	3.907 (1.169–13.058)	.0268
Right superior frontal gyrus, medial orbital	1.230	3.422 (1.213–9.649)	.0200
Right gyrus rectus	1.432	4.186 (1.280–13.693)	.0179
Right medial orbital gyrus	1.157	3.179 (1.076–9.396)	.0365
Right supramarginal gyrus	0.879	2.409 (1.053–5.513)	.0374
Left paracentral lobule	−1.463	0.232 (0.079–0.677)	.0075
Right paracentral lobule	−1.587	0.205 (0.066–0.633)	.0059

Note:—B indicates β coefficient.

difference = 0.7101 (95% CI, −0.0227−1.4429). No significant group differences were observed in networks other than the SMN under the threshold of $P = .05$.

AMS Features Associated with the SMN at High Altitude

Using the multimodal MR imaging scanned at high altitude, we further identified the influence of fMRI predictors (fALFF and DC in SMN) by performing the partial Pearson correlation between fMRI predictors and other modalities of brain MR imaging at high altitude (including the whole-brain GM, WM, CSF, and CBF). At 22 hours after exposure, the fALFF in the SMN was significantly correlated with the percentage changes of CSF volume ($r = 0.3277$ and $P = .0365$, shown in Fig 4*A*). Other brain components except CSF were also examined but showed no significance; these are listed in the Online Supplemental Data.

Moreover, we examined the relationship between fMRI predictors in the SMN and 5 different LLS subscores, which were all measured immediately before MR imaging and at 22 hours at high altitude. In Fig 4*B*, by performing the *t* tests, we found that the group that showed significantly ($P = .0460$) positive fatigue symptoms had lower fALFF in the SMN (mean positive LLS) = −0.2578 (SD, 0.1523), (mean negative LLS) = 0.4186 (SD, 0.3341), group difference = 0.6764 (95% CI,−0.0136−1.3664), and the group whose clinical function was affected had significantly ($P = .0024$) lower fALFF (mean positive LLS) = −0.5836 (SD, 0.1265), (mean negative LLS) = 0.3525 (SD, 0.3214), group difference = 0.9361 (95% CI, 0.3403−1.5320), and significantly ($P = .0112$) lower DC, (mean positive LLS) = −0.5452 (SD, 0.1612), (mean negative LLS) = 0.2380 (SD, 0.2799), group difference = 0.7832 (95% CI, 0.0856−1.4808) in the SMN.

DISCUSSION

Although a previous MR imaging study for AMS[28,29] had detected several brain abnormalities in the diffusion MR imaging after exposure, to the best of our knowledge, our study was the first to perform multimodal MR imaging at sea level and at high altitude for both integrated predicting and mechanistic investigating of AMS. The major findings lie in 2 parts: First, we discovered that sea-level SMN function can predict AMS with a high performance of AUC = 86.4%, which offered a method to predict the AMS risk for individuals requiring rapid ascent to high-altitude areas, such as those undertaking urgent high-altitude missions. Second, we further verified that the predictors also showed significant group difference between AMS and non-AMS at high altitude. The predictors were also associated with the changes in CSF volume and the extent of fatigue and clinical function.

These findings suggest that a cerebral functional basis for AMS can be detected early at sea level and shows promise as a noninvasive and accurate prediction tool and can offer insight into the neural basis of the susceptibility and development of AMS.

Methodologic Considerations for the Reliability of Prediction

We used LASSO-LR for its capability for feature selection (Online Supplemental Data). The selected features remained robust in cross-validation and different coefficient thresholds (Online Supplemental Data). We did not correct multiple comparisons among predictors because we used a data-driven LASSO-LR but did not screen all features. The multiple-comparisons correction might unnecessarily increase the risk of type II errors (false-negatives), thereby hindering the exploring of meaningful predictors. Despite including ASL MR imaging and structural MR imaging at both sites, our exploratory analyses rarely identified significant predictors from these modalities. We observed several ROC curves significantly below the diagonal line. This finding suggests that while these modalities may hold some useful information, they fail to provide robust and reliable predictions, indicating their limited applicability in this context.[34,38] The combined features like all fMRI or all MR imaging features showed insignificant performance (Online Supplemental Data), which indicates that simply combining all features into the prediction model will lead to overfitting and that each type of feature should be tested independently.

AMS Predictors as the Functional Features in the SMN

We found that functional features of fALFF and DC in the SMN were significant predictors for AMS (Table 3). We used both voxelwise and network-wise *t* tests to re-verify these predictors, as shown in Fig 3. The SMN in the predefined brain network atlas[37] broadly includes the primary motor and somatosensory cortices as well as part of the superior temporal gyrus, and these regions match the protective predictors well (Table 3).

For the fALFF and DC as predictors, higher DC in the SMN indicates that the SMN plays a more critical role in facilitating communication and information flow among other brain regions,

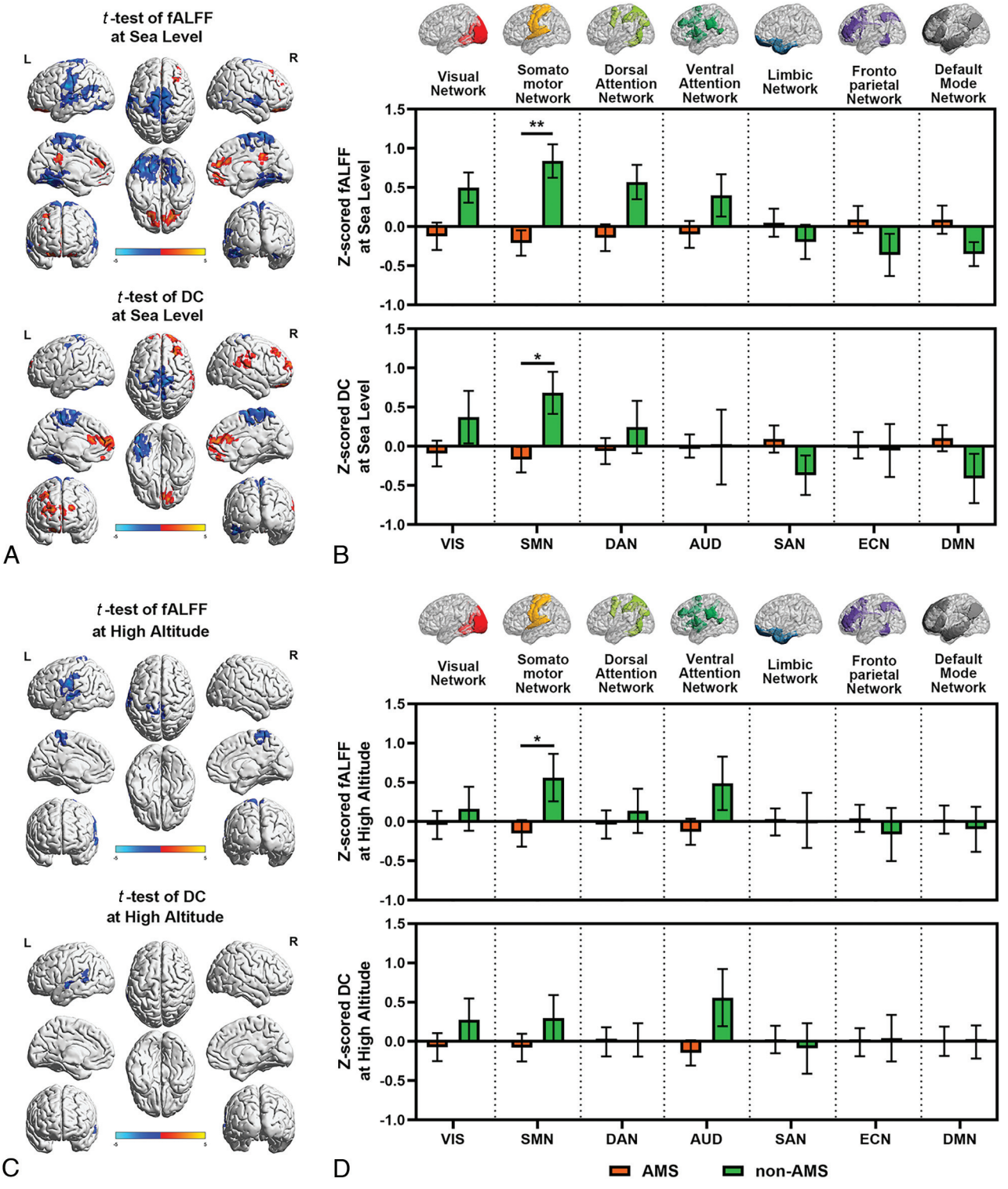

FIG 3. Comparison of functional metrics between AMS and non-AMS groups. *A*, Sea-level voxelwise differences. Differences between AMS and non-AMS groups are identified using *t* tests, corrected with the Gaussian random field at $P < .05$. For both fALFF and DC, AMS showed increased functional metrics in the medial prefrontal cortex, supramarginal gyrus, posterior cingulate cortex, and superior frontal gyrus and decreased functional metrics in the supplementary motor area, postcentral gyrus, paracentral lobule, Rolandic operculum, middle cingulate cortex, and superior temporal gyrus. *B*, Sea-level network-wise differences. Among 7 typical functional networks at sea level, we detected significant lower fALFF and DC in the SMN in the AMS group (*: $P < .05$; **: $P < .01$). The *error bars* present the standard error of the mean (SEM). *C*, High-altitude voxelwise differences. At high altitudes, for both fALFF and DC, AMS showed decreased functional metrics in the postcentral gyrus, Rolandic operculum, and superior temporal gyrus. *D*, High-altitude network-wise differences. Among 7 typical functional networks at high altitude, we detected significant lower fALFF in SMN in the AMS group (*: $P < .05$). The *error bars* present SEM. L indicates left; R, right.

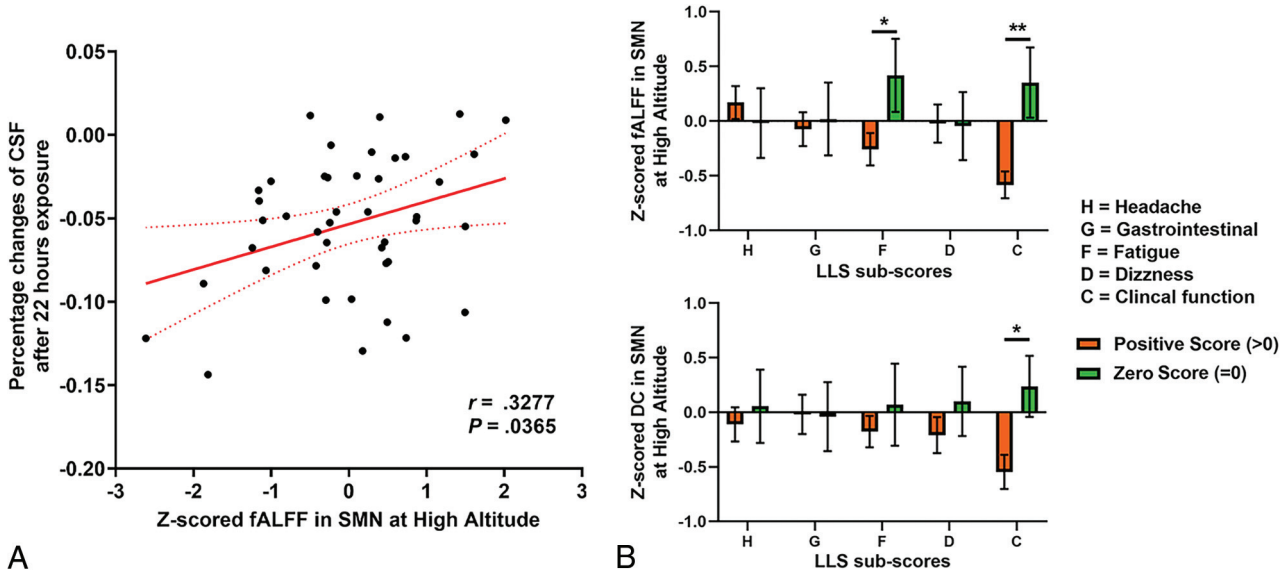

FIG 4. The pathophysiologic impact of sea-level functional predictors on AMS, measured at 22 hours after high-altitude exposure. *A*, Correlation between the fALFF in the SMN and the percentage change in CSF volume. The partial Pearson correlation coefficient is $r = 0.3277$ and $P = .0365$, considering the effects age and sex. *B*, *T* test comparisons show significant differences in fALFF and DC in the SMN between participants having positive LLS subscores and those with zero subscores. The *error bars* present standard error of the mean. The LLS subscores associated with SMN function were fatigue and clinical function scores. * $P < .05$; ** $P < .01$.

while higher fALFF in the SMN means stronger spontaneous neural activity.[39,40] Insignificant regional homogeneity results suggested that AMS might be less related to local synchrony within brain regions. Because weaker SMN function leads to higher AMS probability in this study, resting-state sea-level SMN could potentially indicate the capability for subsequent high-altitude adaptation, showing promise for clinical use. The stronger SMN activity for better adaptation aligns with previous studies, which regard the SMN as regions responsible for integrating sensory signals from the environment, especially for the sensation of hypoxia,[41-43] while hypoxia is a commonly-recognized trigger of AMS.[1] Moreover, the SMN is found to be specifically affected by the brain hypoxia–ischemia injury in the former reports on neonatal rats and humans;[44-46] this finding can also be related to the important role of SMN during the high-altitude hypoxia and the onset of AMS. In summary, we speculated that a functionally more active SMN could imply a more efficient processing and integration of sensory input, indicating protective and adaptive compensatory mechanisms in response to exposure.

The risk factors of AMS in Table 3 and Fig 3*A* were mainly distributed in the orbitofrontal cortex and right supramarginal gyrus, aligning with the sensory processing function that was previously proposed.[47,48] However, these group differences did not remain significant at high altitude (Fig 3*C*). Therefore, this study focused more on the SMN as the most promising protective predictor of AMS.

Identifying the Pathophysiologic Impact of AMS Predictors at High Altitude

At high altitude, a weaker SMN function showed a significant association with less change of CSF volume after exposure (Fig 4*A*). Other modalities of GM, WM, and CBF showed no correlation with SMN function (Online Supplemental Data). Changes in CSF and the saturation of pulse oxygen (SpO_2) are shown in the Online Supplemental Data. This result provides evidence for the differential effects of various brain components at the onset of high-altitude symptoms.[25,27] On the basis of the high-altitude MR imaging, our results propose that among the volume effect of different brain components,[19] CSF is directly related to brain functional activity during AMS, a relationship also observed in a previous study,[49] and we propose a potential mechanism of AMS susceptibility: SMN-based functional predictors might be dynamically associated with AMS by reflecting changes in CSF flow after exposure.

Then, we detected the differences of SMN function between LLS-positive and -negative groups (Fig 4*B*). Although headache is widely believed to be the key factor of AMS,[2] our *t* test analyses suggest that the SMN function might lead to the development of AMS by influencing the levels of fatigue and the clinical function. In detail, the clinical function measures the overall influence extent of the symptoms on the individual's activity. The relationships between weaker SMN function and fatigue or clinical function was formerly confirmed in studies without high-altitude exposure[50,51] and was in line with our results. However, our results further suggest that this mechanism can underlie the onset of AMS.

Overall, we suggest that the functional features of the SMN within the brain serve as early indicators and pathologic features of AMS, which suggests focusing on the functional aspects of the brain in future AMS research.

Potential Clues for Future Treatment and Prevention of AMS

Our SMN-based hypothesis on AMS susceptibility could potentially explain why lower-altitude or hypoxic training before exposure is effective in preventing AMS,[52] as interpreted by the augmentation of SMN functionality during training, because this augmentation

was also observed in training patients with incomplete spinal cord injury.[53] Additionally, the relationship between SMN activity and CSF dynamics or LLS subscores might suggest a potential treatment target. Treatments that modulate CSF volume and flow in response to changes in clinical function or fatigue state could be explored during the development of AMS.

Limitations

Our study had limitations. First, we defined AMS as any diagnosis during the 5 time points at the plateau to achieve a generic prediction for wider populations, but future studies can consider the different onset, duration, and extent of AMS as separate subgroups. Second, all participants are sea-level residents with ages relatively limited to 20–40 years (mean, 28.7 [SD, 4.4] years). Therefore, the generalizability to other age ranges and to residents at high altitude is relatively weaker. However, we selected this age range to minimize the potential confounding effects of age-related brain changes.

CONCLUSIONS

Our multimodal MR imaging study revealed that the SMN function, as detected by sea-level rs-fMRI, emerged as a crucial predictor for AMS among multimodal MR imaging features. Furthermore, we validated its pathophysiologic impact at high altitudes. Although this study is derived from a relatively small sample size of 45 and should be considered as a preliminary feasibility study that requires validation in larger and more diverse populations, these significant findings offer a potential direction for developing a screening tool to predict AMS, particularly for individuals requiring rapid ascent to high-altitude areas, such as those undertaking urgent high-altitude missions, and also offer insight into the underlying mechanisms of AMS at high altitudes.

Disclosure forms provided by the authors are available with the full text and PDF of this article at www.ajnr.org.

REFERENCES

1. Luks AM, Swenson ER, Bärtsch P. **Acute high-altitude sickness**. *Eur Respir Rev* 2017;26:160096 CrossRef Medline
2. Bärtsch P, Swenson ER. **Acute high-altitude illnesses**. *N Engl J Med* 2013;368:2294–302 CrossRef Medline
3. Luks AM, Hackett PH. **Medical conditions and high-altitude travel.** *N Engl J Med* 2022;386:364–73 CrossRef Medline
4. Canoui-Poitrine F, Veerabudun K, Larmignat P, et al. **Risk prediction score for severe high altitude illness: a cohort study.** *PLos One* 2014;9:e100642 CrossRef Medline
5. Burtscher M, Flatz M, Faulhaber M. **Prediction of susceptibility to acute mountain sickness by Sa(O2) values during short-term exposure to hypoxia.** *High Alt Med Biol* 2004;5:335–40 CrossRef Medline
6. Cochand NJ, Wild M, Brugniaux JV, et al. **Sea-level assessment of dynamic cerebral autoregulation predicts susceptibility to acute mountain sickness at high altitude.** *Stroke* 2011;42:3628–30 CrossRef Medline
7. Faulhaber M, Wille M, Gatterer H, et al. **Resting arterial oxygen saturation and breathing frequency as predictors for acute mountain sickness development: a prospective cohort study.** *Sleep Breath* 2014;18:669–74 CrossRef Medline
8. Karinen HM, Peltonen JE, Kahonen M, et al. **Prediction of acute mountain sickness by monitoring arterial oxygen saturation during ascent.** *High Alt Med Biol* 2010;11:325–32 CrossRef Medline
9. Karinen HM, Uusitalo A, Vaha-Ypya H, et al. **Heart rate variability changes at 2400 m altitude predicts acute mountain sickness on further ascent at 3000-4300 m altitudes.** *Front Physiol* 2012;3:336 CrossRef Medline
10. Mandolesi G, Avancini G, Bartesaghi M, et al. **Long-term monitoring of oxygen saturation at altitude can be useful in predicting the subsequent development of moderate-to-severe acute mountain sickness.** *Wilderness Environ Med* 2014;25:384–91 CrossRef Medline
11. Modesti PA, Rapi S, Paniccia R, et al. **Index measured at an intermediate altitude to predict impending acute mountain sickness.** *Med Sci Sports Exerc* 2011;43:1811–18 CrossRef Medline
12. Shen Y, Yang YQ, Liu C, et al. **Association between physiological responses after exercise at low altitude and acute mountain sickness upon ascent is sex-dependent.** *Mil Med Res* 2020;7:53 CrossRef Medline
13. MacInnis MJ, Lohse KR, Strong JK, et al. **Is previous history a reliable predictor for acute mountain sickness susceptibility? A meta-analysis of diagnostic accuracy.** *Br J Sports Med* 2015;49:69–75 CrossRef Medline
14. Chen HC, Lin WL, Wu JY, et al. **Change in oxygen saturation does not predict acute mountain sickness on Jade Mountain.** *Wilderness Environ Med* 2012;23:122–27 CrossRef Medline
15. Small E, Juul N, Pomeranz D, et al. **Predictive capacity of pulmonary function tests for acute mountain sickness.** *High Alt Med Biol* 2021;22:193–200 CrossRef Medline
16. Wagner DR, Knott JR, Fry JP. **Oximetry fails to predict acute mountain sickness or summit success during a rapid ascent to 5640 meters.** *Wilderness Environ Med* 2012;23:114–21 CrossRef Medline
17. Millet GP, Faiss R, Pialoux V. **Point: hypobaric hypoxia induces different physiological responses from normobaric hypoxia.** *J Appl Physiol (1985)* 2012;112:1783–84 CrossRef Medline
18. Meier D, Collet TH, Locatelli I, et al. **Does this patient have acute mountain sickness?: the rational clinical examination systematic review.** *JAMA* 2017;318:1810–19 CrossRef Medline
19. Lawley JS, Alperin N, Bagci AM, et al. **Normobaric hypoxia and symptoms of acute mountain sickness: elevated brain volume and intracranial hypertension.** *Ann Neurol* 2014;75:890–98 CrossRef Medline
20. Zhou Y, Huang X, Zhao T, et al. **Hypoxia augments LPS-induced inflammation and triggers high altitude cerebral edema in mice.** *Brain Behav Immun* 2017;64:266–75 CrossRef Medline
21. Storz JF, Scott GR. **Life ascending: mechanism and process in physiological adaptation to high-altitude hypoxia.** *Annu Rev Ecol Evol Syst* 2019;50:503–26 CrossRef Medline
22. Zhang X, Zhang J. **The human brain in a high-altitude natural environment: a review.** *Front Hum Neurosci* 2022;16:915995 CrossRef Medline
23. Dhar P, Sharma VK, Das SK, et al. **Differential responses of autonomic function in sea level residents, acclimatized lowlanders at >3500 m and Himalayan high altitude natives at >3500 m: a cross-sectional study**. *Respir Physiol Neurobiol* 2018;254:40–48 CrossRef Medline
24. Sander M. **Does the sympathetic nervous system adapt to chronic altitude exposure?** *Adv Exp Med Biol* 2016;903:375–93 CrossRef Medline
25. Wilson MH. **Monro-Kellie 2.0: The dynamic vascular and venous pathophysiological components of intracranial pressure.** *J Cereb Blood Flow Metab* 2016;36:1338–50 CrossRef Medline
26. Wei W, Wang X, Gong Q, et al. **Cortical thickness of Native Tibetans in the Qinghai-Tibetan Plateau.** *AJNR Am J Neuroradiol* 2017;38:553–60 CrossRef Medline
27. Benson JC, Madhavan AA, Cutsforth-Gregory JK, et al. **The Monro-Kellie Doctrine: a review and call for revision.** *AJNR Am J Neuroradiol* 2023;44:2–6 CrossRef Medline
28. Fan C, Zhao Y, Yu Q, et al. **Reversible brain abnormalities in people without signs of mountain sickness during high-altitude exposure.** *Sci Rep* 2016;6:33596 CrossRef Medline

29. Hunt JS, Theilmann RJ, Smith ZM, et al. **Cerebral diffusion and T-2: MRI predictors of acute mountain sickness during sustained high-altitude hypoxia.** *J Cereb Blood Flow Metab* 2013;33:372–80 CrossRef Medline
30. Roach RC, Hackett PH, Oelz O, et al; Lake Louise AMS Score Consensus Committee. **The 2018 Lake Louise Acute Mountain Sickness Score.** *High Alt Med Biol* 2018;19:4–6 CrossRef Medline
31. Rolls ET, Huang CC, Lin CP, et al. **Automated anatomical labelling atlas 3.** *Neuroimage* 2020;206:116189 CrossRef Medline
32. Desikan RS, Segonne F, Fischl B, et al. **An automated labeling system for subdividing the human cerebral cortex on MRI scans into gyral based regions of interest.** *Neuroimage* 2006;31:968–80 CrossRef Medline
33. Tibshirani R. **Regression shrinkage and selection via the Lasso.** *Journal of the Royal Statistical Society: Series B (Methodological)* 1996;58:267–88 CrossRef
34. Fawcett T. **An introduction to ROC analysis.** *Pattern Recognition Letters* 2006;27:861–74. Accessed December 26, 2023 CrossRef
35. Jeni LA, Cohn JF, De La Torre F. **Facing imbalanced data recommendations for the use of performance metrics.** *Int Conf Affect Comput Intell Interact Workshops* 2013;2013:245–51 CrossRef Medline
36. Wang L, Han M, Li X, et al. **Review of classification methods on unbalanced data sets.** *IEEE Access* 2021;9:64606–28. Accessed December 25, 2023 CrossRef
37. Thomas Yeo BT, Krienen FM, Sepulcre J, et al. **The organization of the human cerebral cortex estimated by intrinsic functional connectivity.** *J Neurophysiol* 2011;106:1125–65 CrossRef Medline
38. Flach PA, Wu S. **Repairing concavities in ROC curves.** Internattional Joint Conference on Artificial Intelligence 2005:702–07. https://www.academia.edu/download/35346892/2000402.pdf. Accessed December 26, 2023
39. Zou QH, Zhu CZ, Yang Y, et al. **An improved approach to detection of amplitude of low-frequency fluctuation (ALFF) for resting-state fMRI: Fractional ALFF.** *J Neurosci Methods* 2008;172:137–41 CrossRef Medline
40. Zuo XN, Ehmke R, Mennes M, et al. **Network centrality in the human functional connectome.** *Cereb Cortex* 2012;22:1862–75 CrossRef Medline
41. Legros A, Marshall HR, Beuter A, et al. **Effects of acute hypoxia on postural and kinetic tremor.** *Eur J Appl Physiol [Physiol* 2010;110:109–19 CrossRef Medline
42. Kline DD. **Chronic intermittent hypoxia affects integration of sensory input by neurons in the nucleus tractus solitarii.** *Respir Physiol Neurobiol* 2010;174:29–36 CrossRef Medline
43. LaManna JC, Vendel LM, Farrell RM. **Brain adaptation to chronic hypobaric hypoxia in rats.** *J Appl Physiol (1985)* 1992;72:2238–43 CrossRef Medline
44. Quairiaux C, Sizonenko SV, Mégevand P, et al. **Functional deficit and recovery of developing sensorimotor networks following neonatal hypoxic–ischemic injury in the rat**. *Cereb Cortex* 2010;20:2080–91 CrossRef Medline
45. Wang Y, Wang Y, Hua G, et al. **Changes of functional brain network in neonates with different degrees of hypoxic-ischemic encephalopathy.** *Brain Connect* 2023;13:427–35 CrossRef Medline
46. Jiang L, El-Metwally D, Sours Rhodes C, et al. **Alterations in motor functional connectivity in neonatal hypoxic ischemic encephalopathy.** *Brain Inj* 2022;36:287–94 CrossRef Medline
47. Peng W, Jia Z, Huang X, et al. **Brain structural abnormalities in emotional regulation and sensory processing regions associated with anxious depression.** *Prog Neuropsychopharmacol Biol Psychiatry* 2019;94:109676 CrossRef Medline
48. Kessner SS, Schlemm E, Gerloff C, et al. **Grey and white matter network disruption is associated with sensory deficits after stroke.** *Neuroimage Clin* 2021;31:102698 CrossRef Medline
49. Williams SD, Setzer B, Fultz NE, et al. **Neural activity induced by sensory stimulation can drive large-scale cerebrospinal fluid flow during wakefulness in humans.** *PLoS Biol* 2023;21:e300203 CrossRef Medline
50. Gay CW, Robinson ME, Lai S, et al. **Abnormal resting-state functional connectivity in patients with chronic fatigue syndrome: results of seed and data-driven analyses.** *Brain Connect* 2016;6:48–56 CrossRef Medline
51. Betzel RF, Satterthwaite TD, Gold JI, et al. **Positive affect, surprise, and fatigue are correlates of network flexibility.** *Sci Rep* 2017;7:520 CrossRef Medline
52. Schommer K, Wiesegart N, Menold E, et al. **Training in normobaric hypoxia and its effects on acute mountain sickness after rapid ascent to 4559 m.** *High Alt Med Biol* 2010;11:19–25 CrossRef Medline
53. Trumbower RD, Jayaraman A, Mitchell GS, et al. **Exposure to acute intermittent hypoxia augments somatic motor function in humans with incomplete spinal cord injury.** *Neurorehabil Neural Repair* 2012;26:163–72 CrossRef Medline